Обзор ArXiv/astro-ph, 3-9 марта 2026

От Сильченко О.К.

ArXiv: 2603.04044

Properties of Galaxies with Counter-rotating Stellar Disks in the MaNGA Survey

Min Bao [1,2] Zhenyu Tang,[1,2,*] Yanmei Chen [1,2,†] Yong Shi [3] and Qiusheng Gu [1,2]

[1] *School of Astronomy and Space Science, Nanjing University, Nanjing 210023, China*
[2] *Key Laboratory of Modern Astronomy and Astrophysics (Nanjing University), Ministry of Education, Nanjing 210023, China*
[3] *Department of Astronomy, Westlake University, Hangzhou 310030, Zhejiang Province, China*

ABSTRACT

Gas accretion process can fuel both star formation and black hole activity, playing a critical role in galaxy evolution. The counter-rotating structures are believed to originate from gas accretion, serving as an ideal laboratory for studying its impact on galaxy evolution. Based on the Mapping Nearby Galaxies at Apache Point Observatory (MaNGA) survey, we built a sample of 147 galaxies with counter-rotating stellar disks (CRDs). This is the largest CRD sample to date, accounting for ∼1.5% of the MaNGA survey. For a subset of 138 CRDs, global stellar mass (M_*) and star formation rate (SFR) were measured in reference. We constructed a control sample with similar M_* and SFR but lacking counter-rotating structures. The CRDs relatively exhibit more bulge-dominated morphology, lower molecular gas mass fraction and reside in less dense environment, supporting the hypothesis that they primarily originate from gas accretion. We classified 96 out of 138 CRDs into four types based on their stellar and gas kinematics following the criteria from Bao et al. (2022). There are two additional CRD types: 8 CRDs show misalignment between both stellar disks and gas disk, indicating multiple gas accretion events with differing angular momentum directions; 34 CRDs lack ionized gas emission, showing the highest M_* among all the CRD types, which may represent a final stage of CRD evolution. We compared the radial gradients of gas-phase metallicity and stellar population properties between CRD types, and found that the impact of gas accretion on galaxy evolution primarily depends on the abundance of pre-existing gas in progenitors.

Кинематические способы отождествить CRD

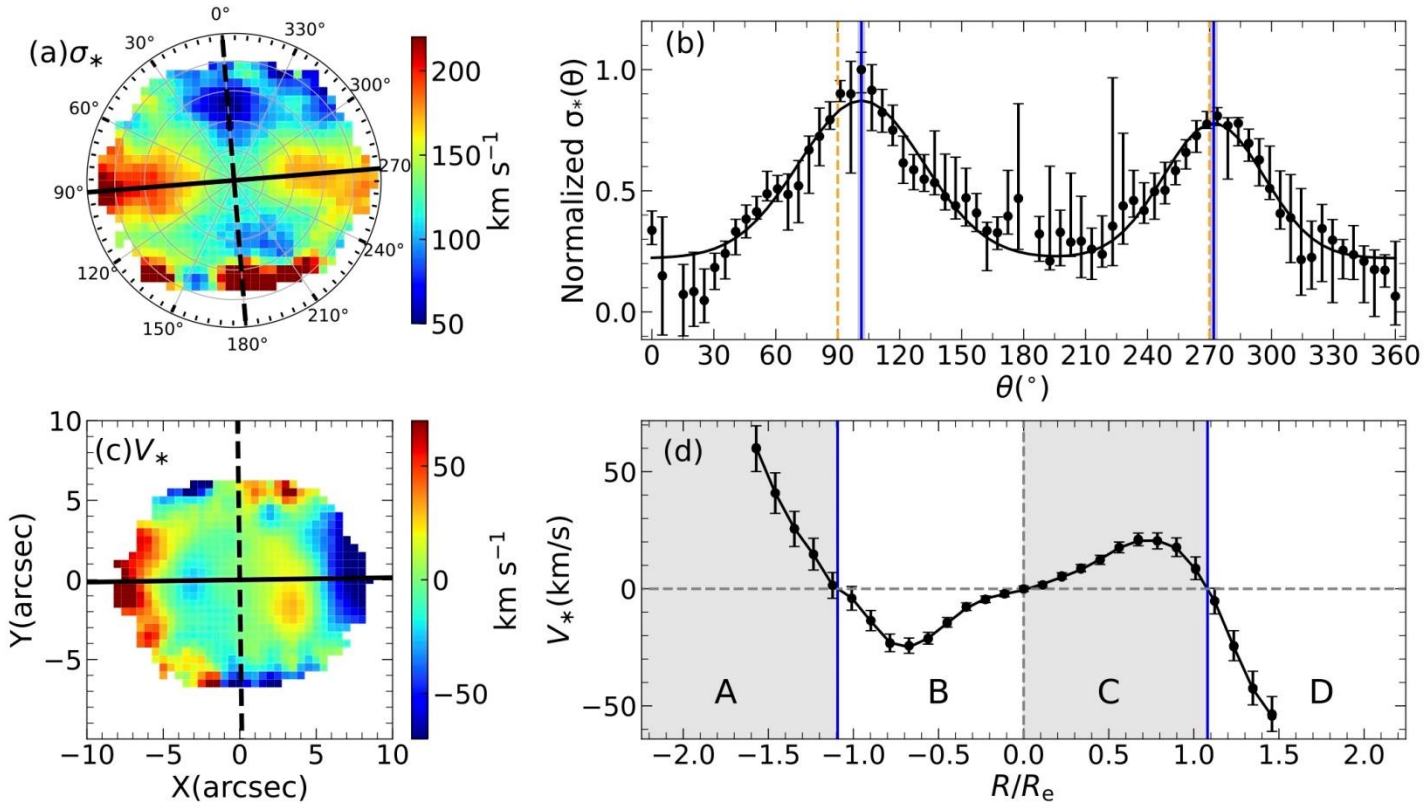

135

45

Figure 1. Two examples of our sample selection. (a) The stellar velocity dispersion field in polar coordinate. The black solid and dashed lines show the photometric major and minor axes. (b) Normalized σ_* as a function of θ. The black circle represents the median σ_* in each sector, with the black vertical bar showing the $\pm 1\sigma$ scattering range. The black curve shows the best-fitting double Gaussian model. The vertical blue lines and grey-shaded areas mark the directions of two peaks and corresponding errors. The vertical orange dashed lines mark $\theta = 90°$ and $\theta = 270°$, the photometric major axis. (c) The stellar velocity field. The black solid and dashed lines show the photometric major and minor axes. (d) v_* along major axis. The black circles show the v_* as a function of radius, with the black vertical bar showing the v_* error. The black curve shows the best result of polynomial fitting. The horizontal grey dashed line marks $v_* = 0$ km s^{-1}. The vertical gray dashed line marks the radius of central velocity-zero point. The vertical blue solid lines mark the radii of the other two velocity-zero points.

Классификация CRD по Min Bao

34

41

17

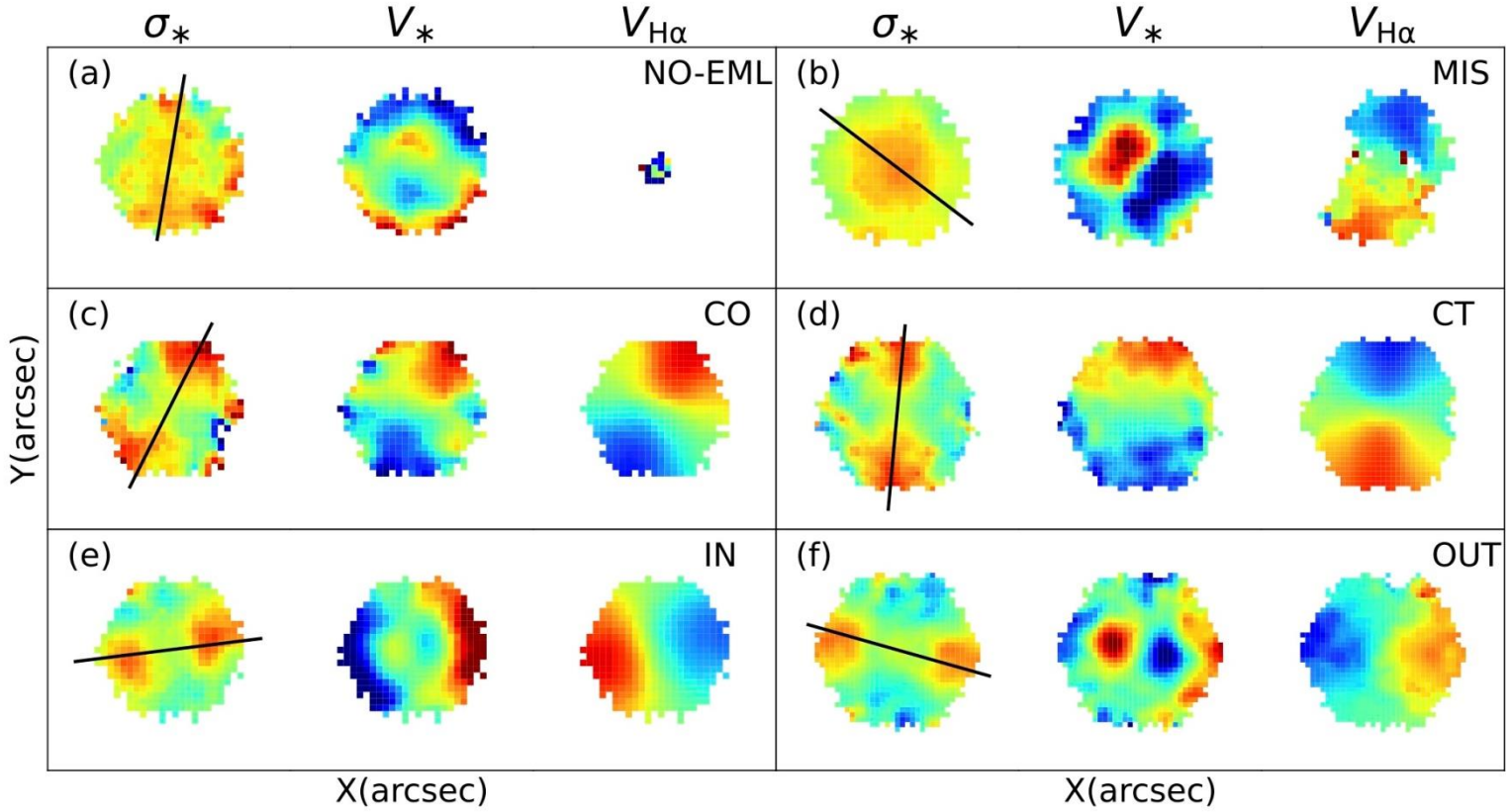

8

25

13

Figure 2. Examples of different types of CRDs. (a) Type NO-EML, where the gas emission can be neglected. (b) Type MIS, where both stellar disks are misaligned with the gas disk. (c) Type CO, where one stellar disk overshines the other, with the brighter stellar disk co-rotating with the gas disk. (d) Type CT, where one stellar disk overshines the other, with the brighter stellar disk counter-rotating with the gas disk. (e) Type IN, where the inner stellar disk is co-rotating with the gas disk. (f) Type OUT, where the outer stellar disk is co-rotating with the gas disk. In all the panels, three subplots sequentially represent stellar velocity dispersion field, stellar velocity field, and gas velocity field traced by Hα. The black solid line in each stellar velocity dispersion field represents the photometric major axis.

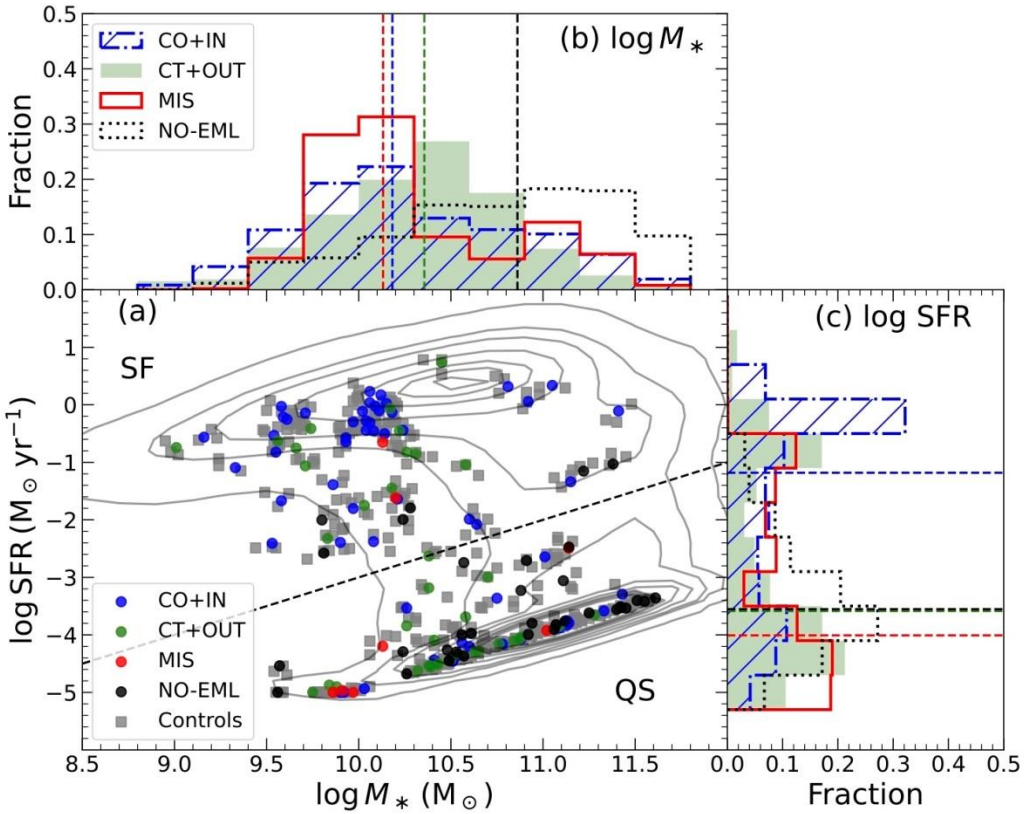

Figure 3. Distribution of CRD sample in the $\log M_*$ - $\log \mathrm{SFR}$ plane. (a) The grey contour shows the distribution of SDSS spectroscopic galaxy sample from Chang et al. (2015) catalog. The blue, green, red and black circles show the distributions of Type CO+IN, Type CT+OUT, Type MIS and Type NO-EML, respectively. The black dashed line classifies galaxies into SF and QS sequence. (b) Distribution of stellar mass. (c) Distribution of star formation rate. In panels (b) and (c), the blue, green, red and black histograms show the M_* and SFR distributions of Type CO+IN, Type CT+OUT, Type MIS and Type NO-EML, respectively. The blue, green, red and black vertical lines show the corresponding median values.

Table 1. The numbers and fractions of SF galaxies for different types of CRDs.

Type of CRDs	Total number	Number of SF galaxies	Fraction of SF galaxies
Type CO+IN	58	39	67.2%
Type CT+OUT	38	14	36.8%
Type MIS	8	2	25.0%
Type NO-EML	34	6	17.6%

Наращивание балджей?

Figure 4 compares the distributions of bulge-to-total ratio between Type CO+IN (panel a), Type CT+OUT (panel b), Type NO-EML (panel c), Type MIS (panel d) and their control samples. In each panel, the colored histogram represents the CRD sample, while the gray histogram represents the control sample. The vertical lines indicate the median values of corresponding distributions.

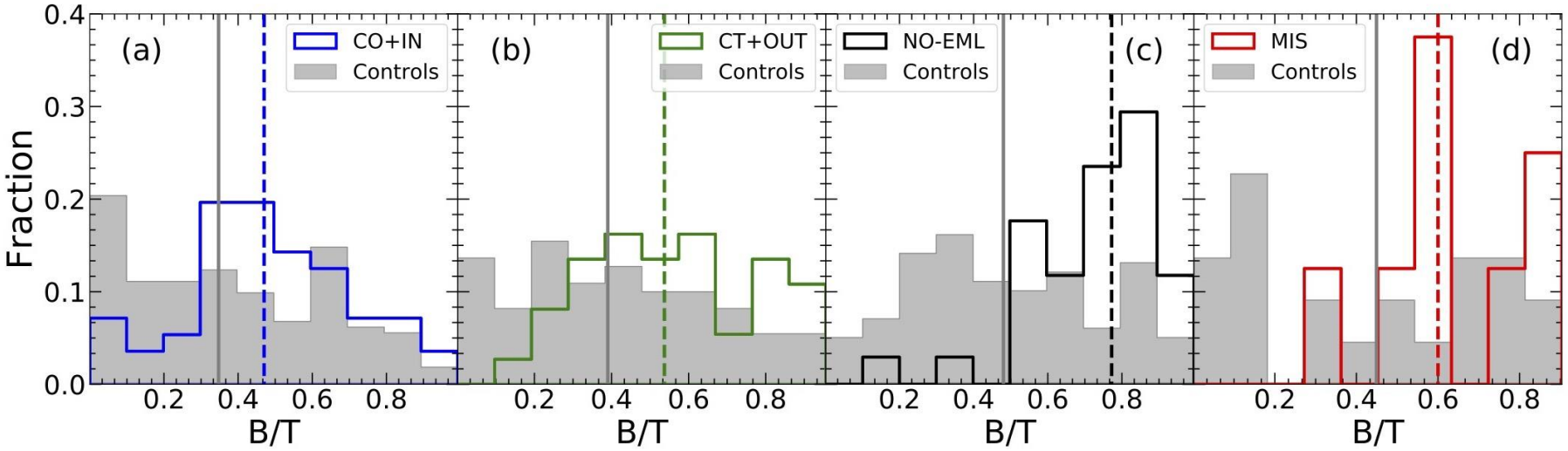

Figure 4. The distributions of bulge-to-total ratio. Four panels sequentially display the B/T distributions for Type CO+IN, Type CT+OUT, Type NO-EML, Type MIS and their control samples. The colorful histograms show the B/T distributions for different CRD types. The grey histograms show the B/T distributions for their control samples. The colorful and grey vertical lines show the corresponding median values.

Бимодальность по молекулярному газу?

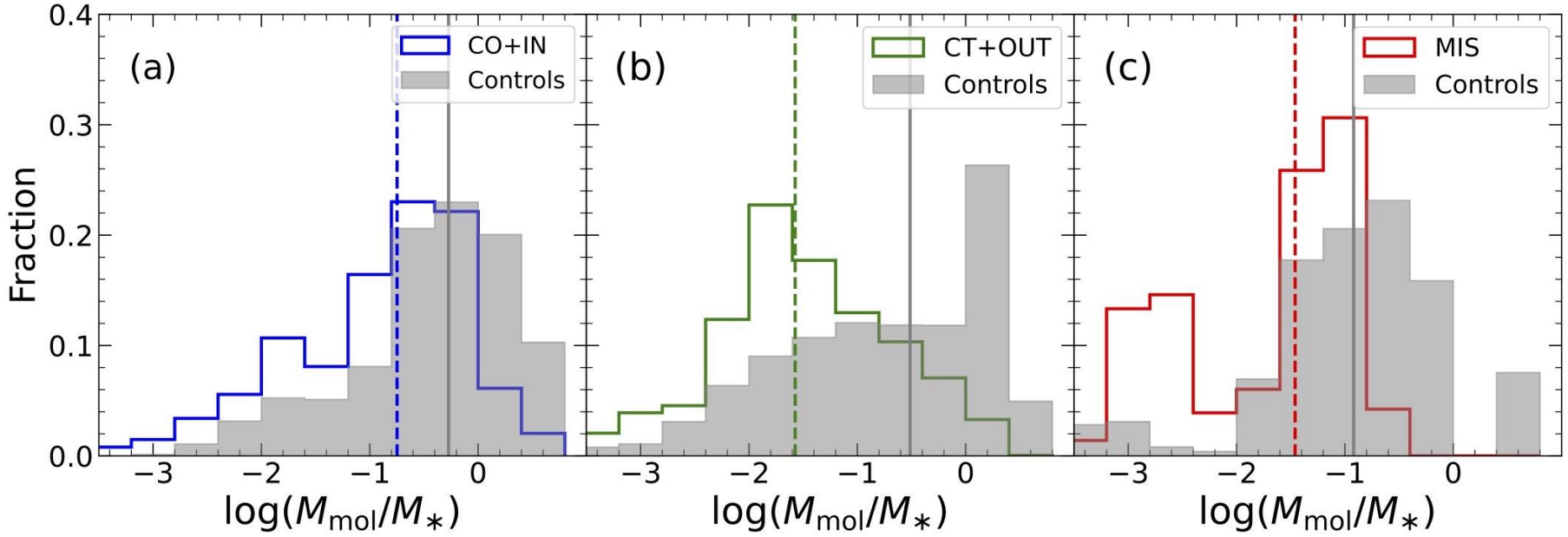

Figure 5. The distributions of molecular gas mass fraction. Three panels sequentially display the $\log(M_{\rm mol}/M_*)$ distributions for Type CO+IN, Type CT+OUT, Type MIS and their control samples. The colorful histograms show the $\log(M_{\rm mol}/M_*)$ distributions for different CRD types. The grey histograms show the $\log(M_{\rm mol}/M_*)$ distributions for their control samples. The colorful and grey vertical lines show the corresponding median values.

Разреженные окрестности?

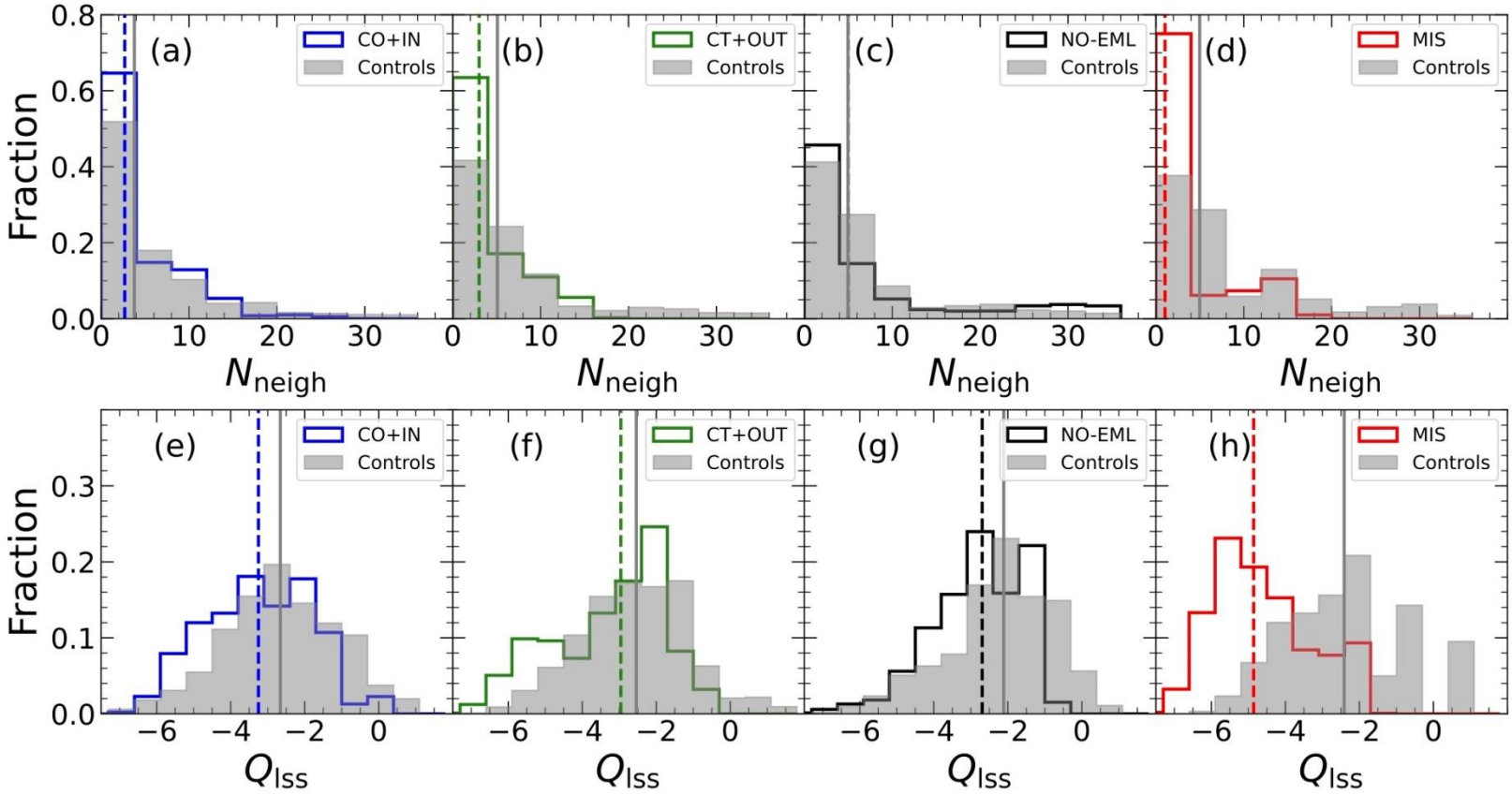

Figure 6. The distributions of environmental parameters. The top and bottom rows display the distributions of neighbour number and tidal strength parameter, respectively. Four panels in each row sequentially display the distributions for Type CO+IN, Type CT+OUT, Type NO-EML, Type MIS and their control samples. The colorful histograms show the distributions for different CRD types. The grey histograms show the distributions for their control samples. The colorful and grey vertical lines show the corresponding median values.

Разные градиенты металличности

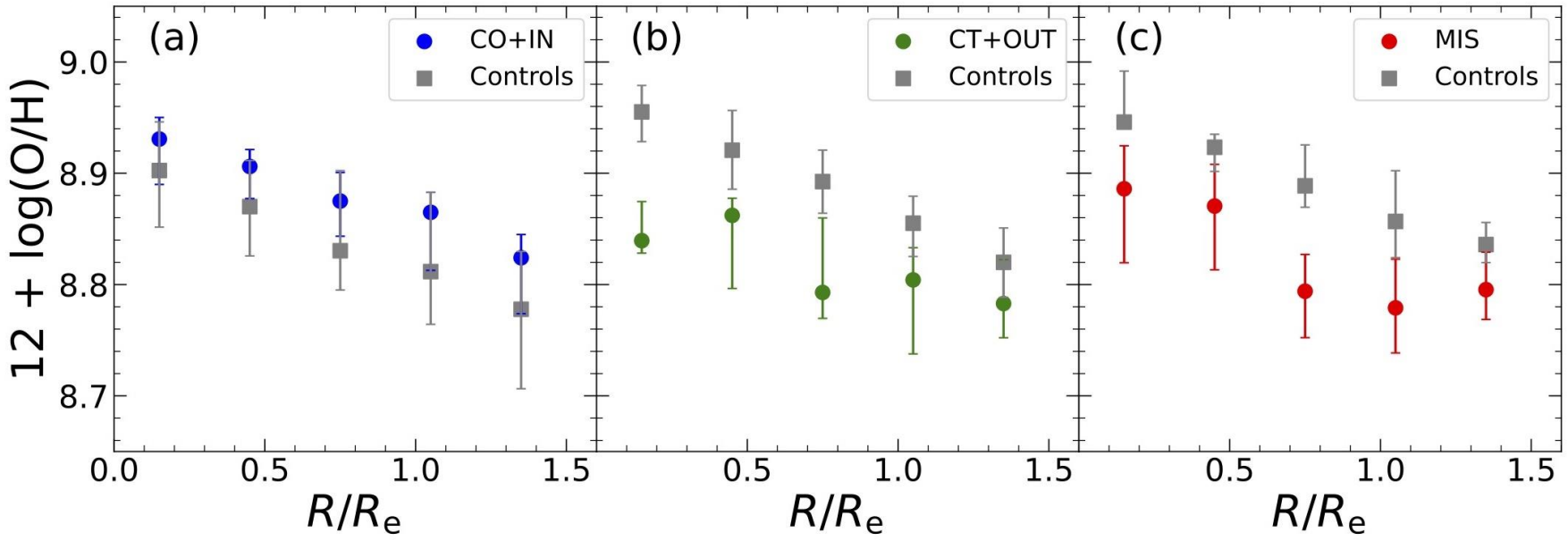

Figure 7. The radial gradients of gas-phase metallicity. Three panels sequentially display the gas-phase metallicity radial gradients for Type CO+IN, Type CT+OUT, Type MIS and their control samples. The colorful circles show the median gas-phase metallicity for different CRD types. The grey squares show the median gas-phase metallicity for their control samples. The colorful and grey error bars show 40%-60% scattering ranges for corresponding radial gradients.

4 галактики, где газ соответствует старому звездному диску

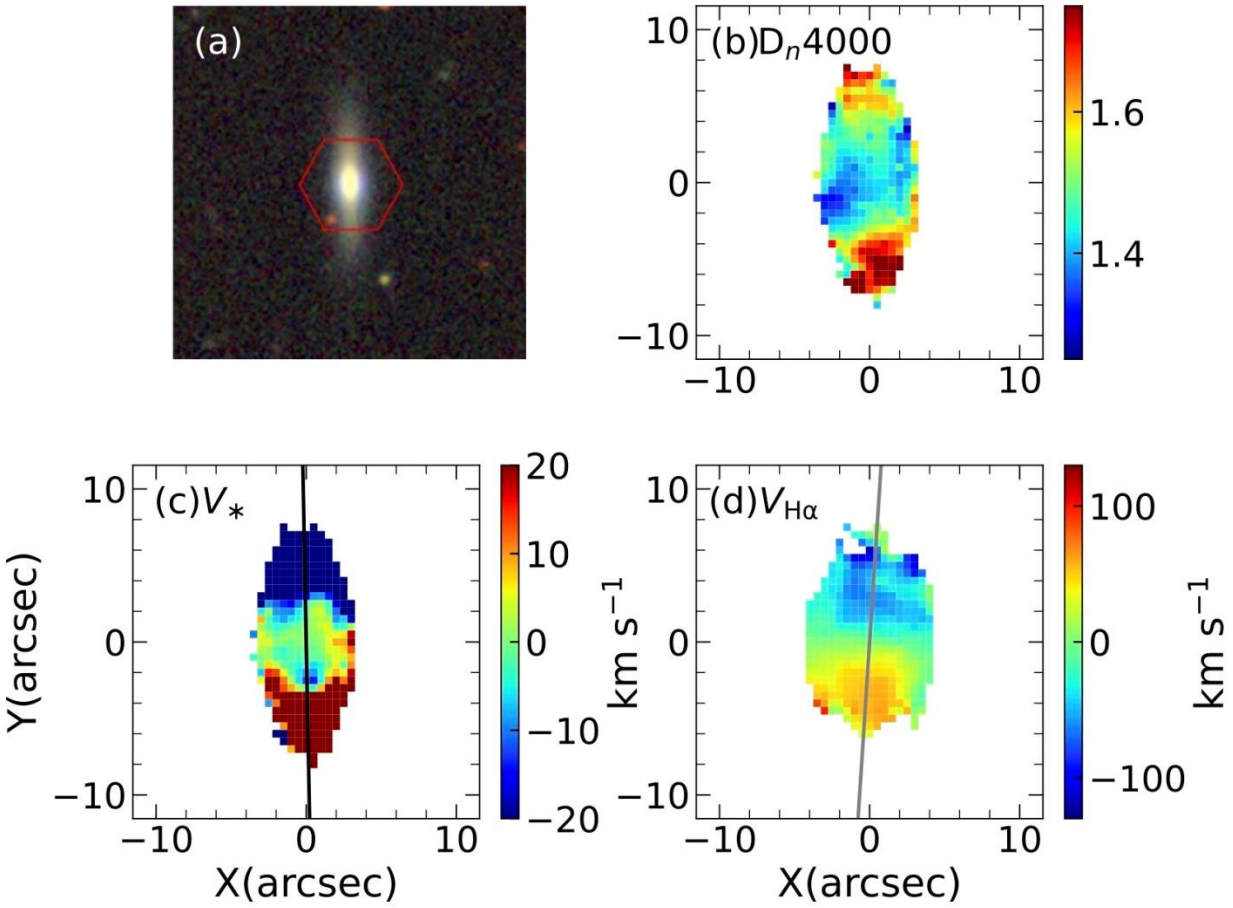

Figure 9. An example for the peculiar CRDs, where the gas disk co-rotates with the older stellar disk. (a) DESI g, r, z composite image. (b) D_n4000 map. Red color shows the relatively older stellar populations, and blue color shows the younger stellar populations. (c) Stellar velocity field. The black solid line shows the kinematic position angle of outer stellar disk. (d) The gas velocity field traced by Hα. The grey solid line shows the kinematic position angle of gas disk.